International Journal of Solids and Structures 49 (2012) 2006–2014

Contents lists available at SciVerse ScienceDirect

International Journal of Solids and Structures

journal homepage: www.elsevier.com/locate/ijsolstr

Homogenization of geomaterials containing voids by random fields and finite elements

D.V. Griffiths [a,b,*], Jumpol Paiboon [a], Jinsong Huang [b], Gordon A. Fenton [c,d]

[a] Department of Civil and Environmental Engineering, Colorado School of Mines, Golden, CO 80401, United States
[b] Australian Research Council Centre of Excellence for Geotechnical Science and Engineering, University of Newcastle, Callaghan NSW 2308, Australia
[c] Department of Engineering Mathematics, Dalhousie University, Halifax, Nova Scotia, Canada B3J 2X4
[d] Faculty of Civil Engineering and Geosciences, Delft University of Technology, 2600 GA Delft, The Netherlands

ARTICLE INFO

Article history:
Received 18 December 2011
Received in revised form 21 March 2012
Available online 13 April 2012

Keywords:
Homogenization
Random finite element method (RFEM)
Representative volume element (RVE)
Effective elastic properties
Foundation analysis
Elastic settlement
Probability and statistics

ABSTRACT

The paper describes the use of random fields and finite elements to assess the influence of porosity and void size on the effective elastic stiffness of geomaterials. A finite element model is developed involving "tied freedoms" that allows analysis of an ideal block of materials leading to direct evaluation of the effective Young's modulus and Poisson's ratio. The influence of block size and representative volume elements (RVE) are discussed. The use of random fields and Monte-Carlo simulations deliver a mean and standard deviation of the elastic parameters that lead naturally to a probabilistic interpretation. The methodology is extended to a foundation problem involving a footing on an elastic foundation containing voids. The approach enables estimates to be made of the probability of excessive settlement.

1. Introduction

The motivation for this work came from a study of foundations resting on subsurface materials containing voids of variable porosity and size (Griffiths et al., 2011a,b). Such sites may consist of a karst topography, which is a special type of landscape and subsurface characterized by the dissolution of soluble rocks, including limestone and dolomite. Even if the expected porosity of the site can be conservatively estimated, the location of the voids may be unknown lending itself to a probabilistic analysis. In addition, two sites with the same porosity may have quite different void sizes, where one has numerous small voids, while the other, fewer large voids. To facilitate modeling of boundary value problems, the goal of this work is to determine the effective elastic parameters of such materials, where the effective values are defined as the Young's modulus and Poisson's ratio (or shear and bulk modulus) that would have led to the same response if the material had been homogeneous.

In this paper, we use the random finite element method (RFEM) (e.g. Fenton and Griffiths, 2008) to examine the influence of voids on the parameters of an elastic material. The method starts with a conventional plane strain FE model of an elastic block of material, after which a random field of values is generated taking account of local averaging (e.g. Fenton and Vanmarcke, 1990) and mapped onto the mesh. The goal of the study is to generate results giving guidance on the mean and standard deviation of the effective Young's modulus and Poisson's ratio as a function of porosity and void size. The parametric studies reported in this paper also give insight into the relationship between the representative volume element (RVE) for a material containing voids and the number of Monte-Carlo simulations needed to reach statistical convergence.

The void volume and size within the specimen is controlled though parameters of the random field as will be explained in the next two sections. Having established the statistical distributions of effective properties as mentioned above, the information can then be applied to more practical boundary value problems. Later in this paper, we consider the influence of voids on the settlement of a strip footing, leading to estimates of the probability of excessive settlement.

The behavior of a heterogeneous material with micro-structure, consisting of varying properties has been studied by a number of investigators. The goal is to obtain the effective or equivalent properties at the macro-scale. An important objective of micro-mechanics is to link mechanical relations going from finer to coarser length scales.

It is assumed that the stiffness parameters of the intact material (e.g. E *and* υ) are known, and the goal of the investigation then becomes one of assessing the macro-stiffness of the material when it is interspersed with voids. A useful concept in this homogenization

* Corresponding author at: Department of Civil and Environmental Engineering, Colorado School of Mines, Golden, CO 80401, United States.
E-mail address: d.v.griffiths@mines.edu (D.V. Griffiths).

0020-7683/$ - see front matter © 2012 Elsevier Ltd. All rights reserved.
http://dx.doi.org/10.1016/j.ijsolstr.2012.04.006

Nomenclature

A	element area
B	footing width
C	settlement proportionality constant
E	effective Young's modulus
E_i	effective Young's modulus at the ith simulation
E_0	Young's modulus of intact material
Δx	element width
Δy	element height
L	width and height of block
n	porosity
$P[\cdot]$	probability
Q	vertical force
x, y	cartesian coordinates
Z	random variable
$z_{n/2}$	value of the standard normal variable
α	dimensionless element size parameter
γ	variance reduction due to local averaging
σ_x	normal stress in x direction
σ_y	normal stress in y direction
σ_z	normal stress in z direction
ε_x	normal strain in x direction
ε_y	normal strain in y direction
δ_x	horizontal deformation
δ_y	vertical deformation
δ_v	vertical deformation in settlement analysis
δ_{vi}	vertical deformation at the ith simulation
θ	spatial correlation length (dimensional)
Θ	spatial correlation length (non-dimensional)
υ	effective Poisson's ratio
μ_{E/E_0}	mean of effective normalized Young's modulus
σ_{E/E_0}	standard deviation of effective normalized Young's modulus
μ	mean
μ_υ	mean of υ
ρ	correlation coefficient
σ, σ^2	standard deviation, variance
$\sigma^2_{(A)}$	variance after local averaging
σ_υ	standard deviation of υ
τ_x, τ_y	difference between x and y coordinates of two points
$\Phi[\cdot]$	standard normal cumulative distribution function

process is the representative volume element or RVE. An RVE is an element of the heterogeneous material that is large enough to capture the effective properties in a reproducible way. From a modeling point of view, the smallest RVE that can achieve this is of particular interest (e.g. Liu, 2005).

The concept of the RVE was first introduced by Hill (1963), since when there have been many numerical simulations developed and applied to determine RVE size (e.g. Kulatilake, 1985; Kanit et al., 2003; Ning et al., 2008; Esmaieli et al., 2010; Huang et al., submitted for publication). Several theoretical models have also been proposed for dealing with scale effects ranging from micro to macro levels. The Differential Method (Roscoe, 1952) has been one of the most effective and widely used methods. The Composite Spheres Model (Hashin, 1962) considered only a single inclusion and led to simple closed-form expressions. The Self Consistent Method (Budiansky, 1965; Hill, 1965) and the Generalized Self Consistent Method, formalized by Christensen and Lo (1979) involved embedding an inclusion phase directly into an infinite medium. Christensen and Lo (1979) explained that the final form of this method can solve the spherical inclusion problem. Finally, the Mori and Tanaka (1973) method as described by Benveniste (1987) has attracted a lot of interest and involves quite complex manipulations of the field variables along with special concepts of strain and stress. Although there are many analytical models for estimating the effective elastic properties of a material containing voids, they are often limited to voids with simple shapes. See also the review of Klusemann and Svendsen (2009).

Numerical methods such as the finite element method (FEM) or the boundary element method (BEM) have been used to validate some of the theoretical approaches. Two major variables can be investigated in a realistic representation of a defective material; namely the volume and size of the voids or inclusions. Isida and Igawa (1991) considered several kinds of periodic arrays of holes, while Day et al. (1992) considered a material containing circular holes within a triangular or hexagonal matrix and occasionally over-lapping random circular holes. Hu et al. (2000) developed a numerical model based on BEM to estimate effective elastic properties such as Young's modulus, bulk modulus and shear modulus. The main objective was to investigate the influence of the shortest distance between holes of random size and volume based on a normal distribution. Cosmi (2004) introduced a new numerical model called the Cell Method (CM) to investigate the effect of randomly located voids. The model consisted of a homogeneous matrix of cells which contains randomly located voids. Li et al. (2010) developed an FEM model to calculate the elastic properties of porous materials with randomly distributed voids.

2. Finite element model

Assuming consistent units, the initial finite element mesh for this study (e.g. Smith and Griffiths, 2004) considers a square plane strain block of material modeled by 50×50 8-node square elements of unit side length ($\Delta x = \Delta y = 1$) as shown in Fig. 1. The boundary conditions allow vertical movement only of nodes on the left side, horizontal movement only of nodes on the bottom side, with the bottom-left corner node fixed. The vertical components of all nodal freedoms on the top loaded side are "tied", as are the horizontal components of all nodal freedoms on the right side. Tied freedoms are forced to move by the same amount in the analysis because they are assigned the same freedom number during stiffness assembly. The tied freedom approach offers an elegant way of modeling a heterogeneous medium as an ideal element of material. The tied freedom approach ensures that the square deforms into a rectangle. Other methods employing stress or strain control may give similar outcomes, but the proposed tied freedom approach, while resulting in neither uniform stresses nor strains within the block, allows an exact back-calculation of equivalent elastic parameters as will be described.

A vertical force shown as $Q = 50$ in the figure is applied to the tied vertical freedom on the top of the square imposing an average unit vertical pressure of $Q/L = 1$. The boundary conditions ensure that no matter what degree of heterogeneity is introduced, such as, for example, the darker regions in Fig. 1 indicating voids, the mesh will always deform as an ideal element with the top surface remaining horizontal and the right side remaining vertical. From

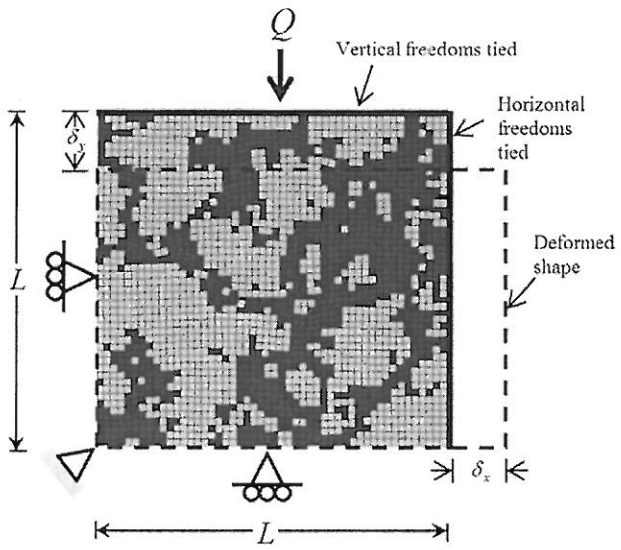

Fig. 1. Tied freedom model with random voids portrayed by the darker zones.

these vertical and horizontal movements under the application of a vertical pressure, the effective Young's modulus and Poisson's ratio can be easily back-figured from linear elastic theory.

These specific boundary conditions enable more direct comparison with experimental results, where displacements may be applied without friction on all sides of the specimen. It is recognized that periodic boundary conditions are often used in homogenization of heterogeneous media, but this is not necessary unless the microstructures are also periodic (e.g. Garboczi and Day, 2005).

The finite element and random field software used in the current work were adapted from the public-domain free software described in the texts by Smith and Griffiths (2004)[1] and Fenton and Griffiths (2008).[2]

3. Local averaging

Input to the analysis consists of the target porosity n and spatial correlation length θ, with the latter offering some control over the void size. A standard normal random variable Z (mean zero and standard deviation of unity at the point level) is assigned to the mesh, with each element receiving a constant value (i.e. there is no variation assumed within an individual element). The spatial correlation length θ is the distance over which values of Z tend to have similar values. The random field generation used in this paper properly accounts for local averaging, which is to say that the unit point variance of the random field is reduced as a function of the ratio $\Delta x/\theta$ prior to mapping onto the mesh. After local averaging, the variance of the standard normal distribution actually mapped onto the mesh will inevitably be less than unity.

In the current work, square elements have been used throughout facilitating mapping of the locally averaged random field onto the mesh (e.g. Fenton and Griffiths, 2008). A disadvantage of the uniform mesh discretization in boundary value problems is that the mesh tends to be "over-refined" in some areas of the problem that would typically be assigned larger elements. Saving are possible by adopting different averaging scales (e.g. Der Kiureghian and Zhang, 1999), however this has not been implemented in the present work in the interests of simplicity. These efficiency considerations may become essential in 3D analysis however, and is left for future work.

When dealing with a normal distribution, local averaging leaves the mean (μ) unchanged, but causes the variance (σ^2) to fall. The larger the finite element size (Δx) relative to the spatial correlation length (θ), the greater the reduction in variance. A further consideration is the nature of the correlation function, which models the way in which the correlation (ρ) between values at any two points in a random field reduces as they move further apart. In the current work, a Markov spatial correlation function has been assumed given by

$$\rho = \exp\left\{-\frac{2}{\theta}\sqrt{\tau_x^2 + \tau_y^2}\right\} \tag{1}$$

where τ_x and τ_y are, respectively, the differences between the x- and y-coordinates of any two points. The variance reduction due to local averaging is defined as

$$\gamma = \frac{\sigma^2_{(A)}}{\sigma^2} \tag{2}$$

where $\sigma^2_{(A)}$ is the locally averaged variance across the area (A) of the finite element. It can be shown (Vanmarcke, 1984) that for a 2D isotropic spatially correlation field acting over a square element of side length

$$\Delta x = \Delta y = \alpha\theta \tag{3}$$

the variance reduction factor is given by

$$\gamma = \frac{4}{\alpha^4}\int_0^{\alpha}\int_0^{\alpha} \exp\left\{-2\sqrt{x^2+y^2}\right\}(\alpha - x)(\alpha - y)dxdy \tag{4}$$

which can be evaluated by numerical integration.

For example, a square element of side length $\theta(\alpha = 1)$ will result in significant variance reduction due to local averaging from Eq. (4) of $\gamma \approx 0.40$. If the element is much smaller than $\theta(\alpha \to 0)$, there will be virtually no variance reduction ($\gamma \to 1$). Conversely, if the element size is much bigger than $\theta(\alpha \to \infty)$, there will be very significant variance reduction ($\gamma \to 0$). Clearly, modeling of small scales of fluctuation will benefit from correspondingly refined finite element meshes. In parametric studies performed in this paper, $\alpha \leqslant 0.2$, so the maximum variance reduction due to local averaging should be less than 20% (see e.g. Griffiths and Fenton, 2004).

4. Porosity model

Once the standard normal random field values have been assigned to the mesh, cumulative distribution tables (suitably digitized in the software) are then used to estimate the value of the standard normal variable $z_{n/2}$ for which

$$\Phi(z_{n/2}) - \Phi(0) = n/2 \tag{5}$$

as shown in Fig. 2. Thereafter, any element assigned a random field value in the range $|Z| > z_{n/2}$ is treated as intact material with Young's modulus and Poisson's ratio of $E_0 = 1$ and $\upsilon_0 = 0.3$, respectively, while any element where $|Z| \leqslant z_{n/2}$ is treated as a void element with an assigned Young's modulus of $E = 0.01$ (100 times smaller than the surrounding intact material). The Poisson's ratio of the voids is maintained at 0.3, although it has been shown that this value has little influence on the statistics of the effective Young's modulus.

5. Void size model

As mentioned previously, the random field spatial correlation length θ offers some quantitative control of void size. By changing the value of θ in the parametric studies, the degree to which void elements with random values in the range $|Z| \leqslant z_{n/2}$ tend to be clustered together can be influenced. A small value of θ will imply

[1] www.mines.edu/~vgriffit/4th_ed.
[2] www.mines.edu/~vgriffit/rfem.

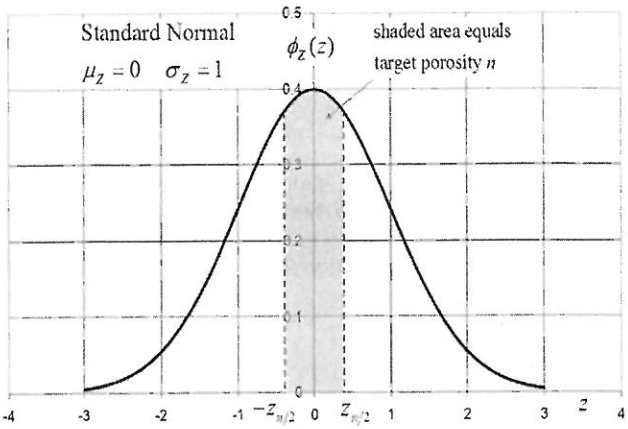

Fig. 2. Target porosity area in standard normal random field.

fewer adjacent elements meeting the criterion at a given location, and hence smaller and more frequent voids, while a large value of θ will imply larger and less frequent voids as shown in Fig. 3.

It should be emphasized that the nature of random fields is such that it is only the average porosity that is under user control. The porosity of each individual simulation such as those shown in Fig. 3 throughout the Monte-Carlo process will vary. This is particularly noticeable when modeling random fields with higher spatial correlation length, in which some individual simulations may display significantly higher or lower porosities than the target value.

In this paper, results have been expressed in terms of a dimensionless spatial correlation length

$$\Theta = \frac{\theta}{L} \tag{6}$$

where L is the width of the loaded block in Fig. 1.

6. Monte-Carlo simulations

A "Monte-Carlo" process means that analyses are repeated numerous times until the statistical properties of the output parameters become acceptably reproducible. In this work, each Monte-Carlo simulation involves the generation of a random field and void distribution as explained previously. This is followed by an elastic analysis of the block such as that shown in Fig. 1. The primary outputs from each elastic analysis are the vertical and horizontal deformations of the block, δ_y and δ_x, respectively. Although each simulation is based on the same θ and n, the spatial location of the voids will be different each time, thus in some cases the voids may occur just below the top of the block leading to a relatively high δ_y while in others, the voids may be buried in the middle of the block leading to a relatively low δ_y.

Following each simulation, the computed displacements δ_y and δ_x are converted into "effective" values of Young's modulus and Poisson's ratio as follows.

From Hooke's Law, where x and y represent respectively the horizontal and vertical directions with z as the out-of-plane direction:

$$\begin{aligned} \varepsilon_x &= \frac{1}{E}(\sigma_x - \upsilon(\sigma_y + \sigma_z)) \\ \varepsilon_y &= \frac{1}{E}(\sigma_y - \upsilon(\sigma_z + \sigma_x)) \end{aligned} \tag{7}$$

Assuming plane strain conditions where $\varepsilon_z = 0$,

$$\sigma_z = \upsilon(\sigma_x + \sigma_y) \tag{8}$$

hence Eq. (7) can be written as

$$\begin{aligned} \varepsilon_x &= \frac{1}{E}(\sigma_x - \upsilon(\sigma_y + \upsilon(\sigma_x + \sigma_y))) \\ \varepsilon_y &= \frac{1}{E}(\sigma_y - \upsilon(\upsilon(\sigma_x + \sigma_y) + \sigma_x)) \end{aligned} \tag{9}$$

For the unconfined axially loaded unit square shown in Fig. 1, $\varepsilon_x = \delta_x/L$, $\varepsilon_y = \delta_y/L$, $\sigma_x = 0.0$ and $\sigma_y = Q/L$, hence after substitution into Eq. (9) and rearrangement

$$\upsilon = \frac{\delta_x}{\delta_x + \delta_y} \tag{10}$$

$$E = \frac{Q(1-\upsilon^2)}{\delta_y} \tag{11}$$

Each Monte-Carlo simulation leads to different block deformations δ_x and δ_y, and hence different values of Young's modulus and Poisson's ratio from Eqs. (10), (11). The Young's modulus E computed at each simulation can be normalized as E/E_0 by dividing by the intact material Young's modulus ($E_0 = 1$).

7. Results of RFEM

The number of Monte-Carlo simulations needed to achieve reasonably reproducible output statistics without excessive computational effort was studied by observing the value of the mean effective Young's modulus over an ever increasing number of simulations as shown in Fig. 4. Following this study, it was decided

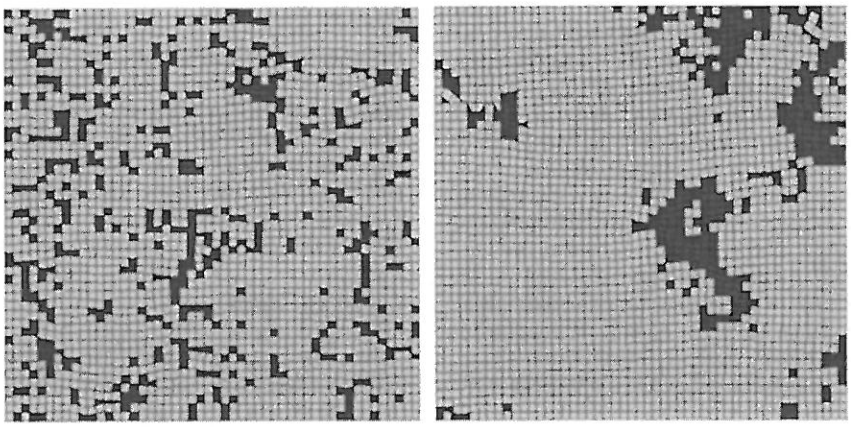

Fig. 3. Typical simulations showing generation of voids at low and high spatial correlation lengths ($n = 0.2$ in both cases).

that 1000 simulations for each parametric combination would be a reasonable compromise.

The mean and standard deviation of the normalized Young's modulus was computed for a range of parametric variations of n and Θ, with results shown in Figs. 5 and 6, respectively. It was noted that very similar plots to those shown in Fig. 5 would be obtained if the shear or bulk modulus had been plotted instead of Young's modulus.

As might be expected from Fig. 5, the mean effective Young's modulus drops towards zero with increasing porosity n. It is also apparent that Θ does not have much influence on μ_{E/E_0}. Fig. 6 shows that Θ has more influence on the standard deviation of the effective Young's modulus σ_{E/E_0}. The standard deviation curves exhibit zero variance for $n \approx 0$ and $n \approx 1$ since these correspond, respectively, to materials with essentially intact stiffness or zero stiffness. As expected therefore, maxima occur in the standard deviation plots at intermediate values of porosity ($n \approx 0.3$).

The mean and standard deviation of Poisson's ratio for the same parametric variations of n and Θ are shown in Figs. 7 and 8 respectively. It can be noted from Fig. 7 that the mean Poisson's ratio μ_υ remains quite constant with a small reduction at intermediate values of n. As shown in Fig. 8, the standard deviation of Poisson's ratio is quite small for all porosities, but again exhibits a maxima, this time at around $n \approx 0.5$.

8. Computer resources and timings

All results presented in this paper were performed on a 50 × 50 mesh using an Intel Core i7-2600 CPU @ 3.40 GHz RAM: 8 GB laptop. Timings for 1000 Monte-Carlo simulations are shown in Fig. 9 for 2D meshes with up to 100 elements on each side (total number of 10,000 elements). The CPU time for a 50 × 50 mesh was about 1.6 h, while a 100 × 100 mesh took 23.2 h. The results of sensitivity studies with two different levels of mesh refinement are shown in Figs. 10 and 11 for the case when $\Theta = 0.5$. The results show a small influence due to mesh refinement, however the difference does not justify the additional computer time required for a comprehensive parametric investigation with the finer mesh.

9. Comparison with other solutions

The current results using the $\Theta = 0.5$ data from the block analyses given in Fig. 5, are now compared with existing theoretical and numerical approaches. From Fig. 12, it can be observed that the current method tends to give lower values of the effective Young's modulus than the theoretical methods of Roscoe (1952),

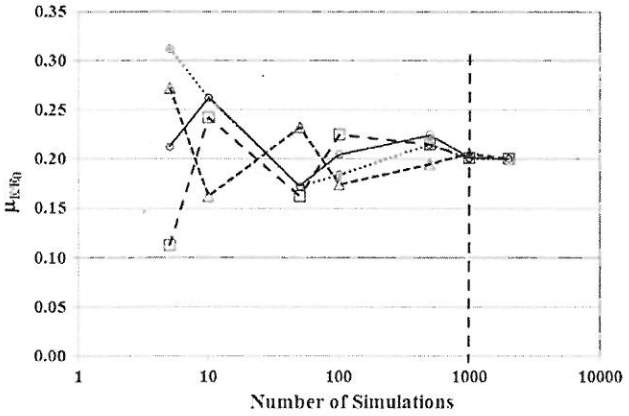

Fig. 4. Influence of the number of simulations on the computed value of the mean effective stiffness for $n = 0.3$ and $\Theta = 0.1$. Runs repeated four times.

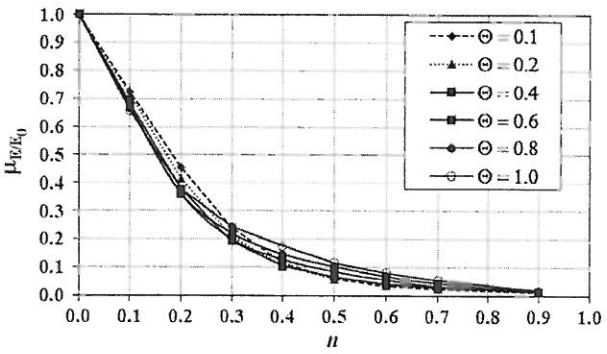

Fig. 5. Mean effective stiffness vs. porosity.

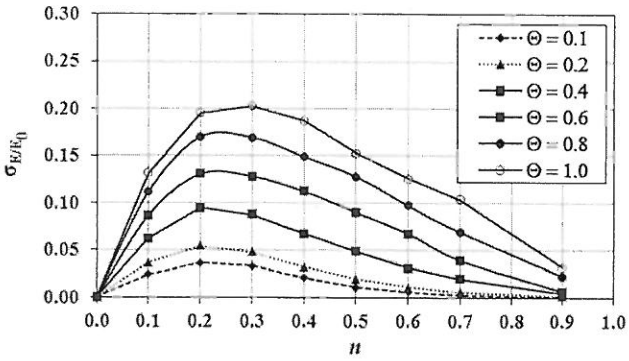

Fig. 6. Standard deviation of effective stiffness vs. porosity.

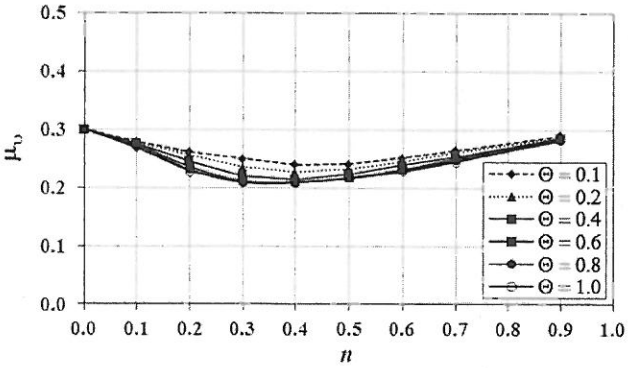

Fig. 7. Mean Poisson's ratio vs. porosity.

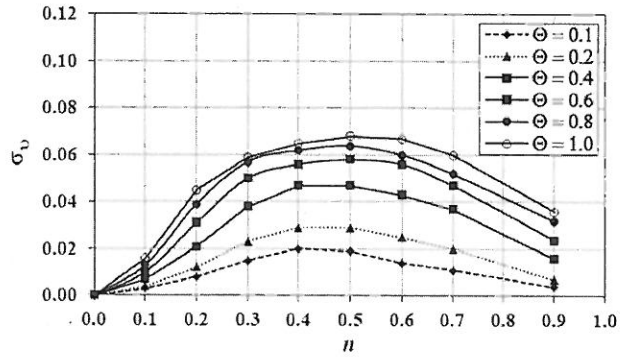

Fig. 8. Standard deviation of Poisson's ratio vs. porosity.

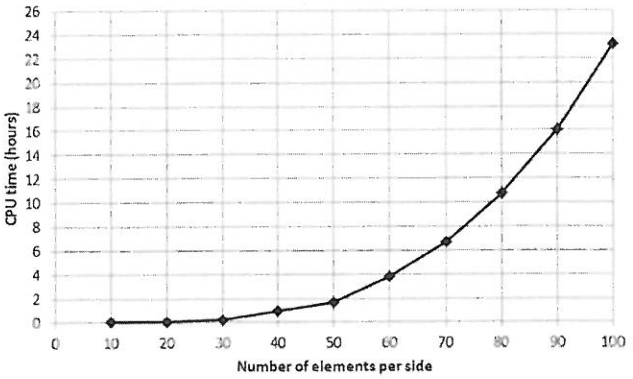

Fig. 9. CPU timings for 1000 Monte-Carlo simulations for different element refinements.

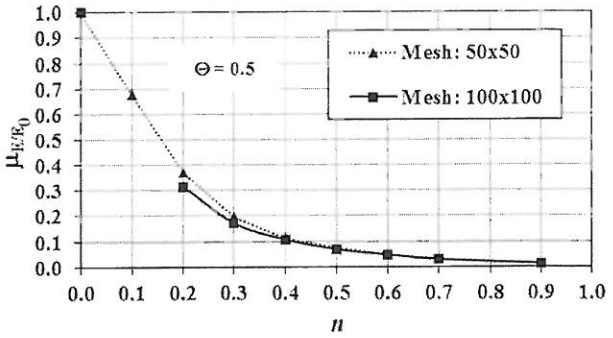

Fig. 10. Influence of mesh refinement on mean effective stiffness.

Mori and Tanaka (1973) and Christensen and Lo (1979) described previously. Fig. 13 shows a comparison between the current method and numerical results of Isida and Igawa (1991) and Day et al. (1992). Once more, the current method tends to give lower values of the effective Young's modulus for nearly all values of n.

The lower values generated by the RFEM results suggest that the existing methods may be optimistic about the homogenized stiffness. The reasons for the differences remain under investigation, but it should be noted that the current method includes control of void size through the random field spatial correlation length, a feature that has not been properly accounted for in earlier work.

10. Representative volume element (RVE)

Although the block analyses presented earlier used a 50 × 50 block of material, it may be asked whether this can be considered a representative volume element (RVE). Is there a smaller block of material that could also deliver an acceptable value of the effective Young's modulus? It may also be expected that a smaller block of material containing voids will require more Monte-Carlo simulations to achieve stable output than a larger block with the same average void structure. Fig. 14 shows a sequence of blocks within a parent block of 100 × 100 square elements of unit side length. The 50 × 50 block considered earlier in this paper was a subset of the parent block.

Tied freedom analyses on a range of block sizes were performed on a material with $n = 0.2$ and $\theta = 20$ .The number of Monte-Carlo simulations was maintained at 1000 in each case.

For the smallest 1 × 1 block model in which each block is the size of a single element, the statistics as shown in Fig. 15 are governed by a Bernoulli process in which, $\mu_{E/E_0} = (1 - n)$ and $\sigma_{E/E_0} = \sqrt{n(1-n)}$. For the case where $n = 0.2$, these become $\mu_{E/E_0} = 0.8$ and $\sigma_{E/E_0} = 0.4$. As the block size increases, it can be noted that the mean Young's modulus falls rapidly at first and then more gradually, and has become essentially constant for block sizes $\geqslant 30 \times 30$. Similarly the standard deviation tends to zero as the block size gets bigger. One could expect that if the block is large enough, each simulation would give an almost identical result. This effect is shown in Fig. 16 where the variation of mean Young's modulus is plotted against the number of Monte-Carlo simulations corresponding to 20 × 20 and 50 × 50 blocks for three repeated analyses.

For the smaller 20 × 20 block in Fig. 16(a) the effective Young's modulus takes at least 500 simulations to stabilize, while the larger 50 × 50 block in Fig. 16(b) settles down in around 100. As expected from Fig. 16, the larger block gives a slightly smaller value of the effective stiffness. The choice of the RVE should be put in the context of the application being considered and the accuracy required. It was also observed that material with voids based on larger spatial correlation lengths required larger block sizes for convergence within a given number of iterations. Since the results in this paper indicate a second order influence of θ on effective elastic properties, further results relating to θ have not been included here.

11. Foundation settlement

The methodology described is now used to study the influence of voids on the settlement of a strip footing using the mesh and properties shown in Fig. 17.

The foundation sub-soil was modelled using 50 × 30 square planar 8-node finite elements of unit side length with Young's modulus $E_0 = 50$ MPa and Poisson's ratio $\upsilon = 0.3$. The strip footing at the ground surface had a width $B = 10$ m and was loaded with a force of $Q = 0.2$ MN. The vertical and horizontal freedoms of the 21 nodes under the footing were tied, ensuring translational movement only (no rotation), and is equivalent to a rough rigid interface. For a uniform foundation with no voids, the computed vertical displacement of $\delta_v = 0.0432$ m was in good agreement with independent solutions (e.g. Sudret and Der Kiureghian, 2000). It may be noted that the vertical displacement of a rigid footing is approximately the same as the average settlement of the centre and edge of a flexible footing carrying the same total load (Davis and Taylor, 1962; Poulos and Davis, 1974). From the uniform validation example and assuming a deterministic Poisson's ratio, the constant of proportionality relating the reciprocal of the effective Young's modulus to vertical footing displacement given by

$$\delta_v = \frac{C}{E} \tag{12}$$

was found to be $C = 2.16$ MN/m.

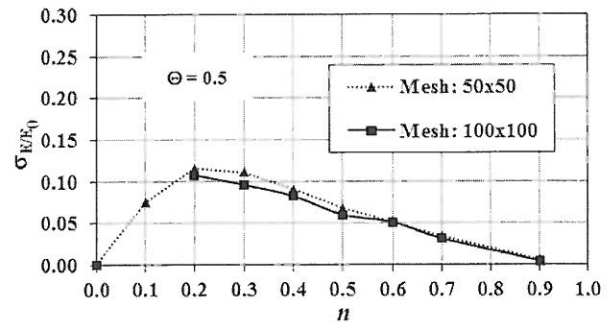

Fig. 11. Influence of mesh refinement on standard deviation of effective stiffness.

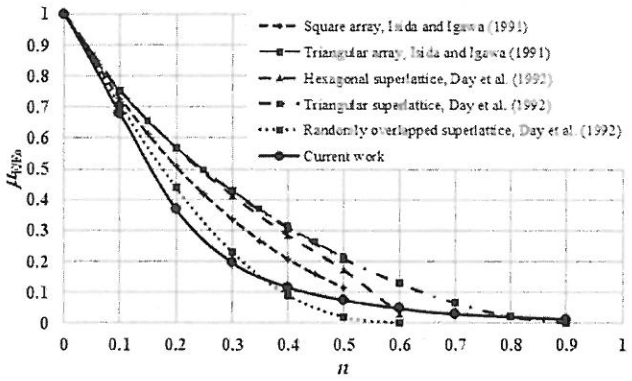

Fig. 12. Comparison of the mean effective Young's modulus obtained from RFEM and different theoretical models.

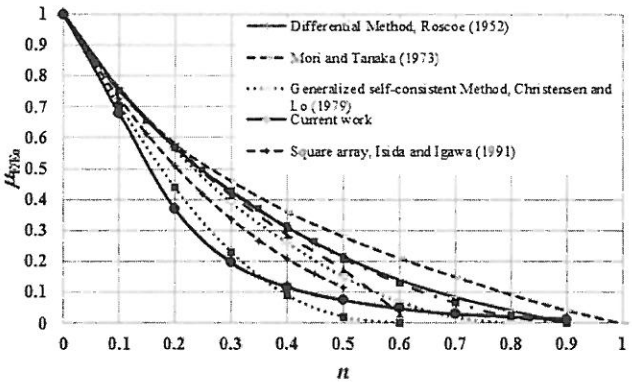

Fig. 13. Comparison of the mean effective Young's modulus obtained from RFEM and different numerical models.

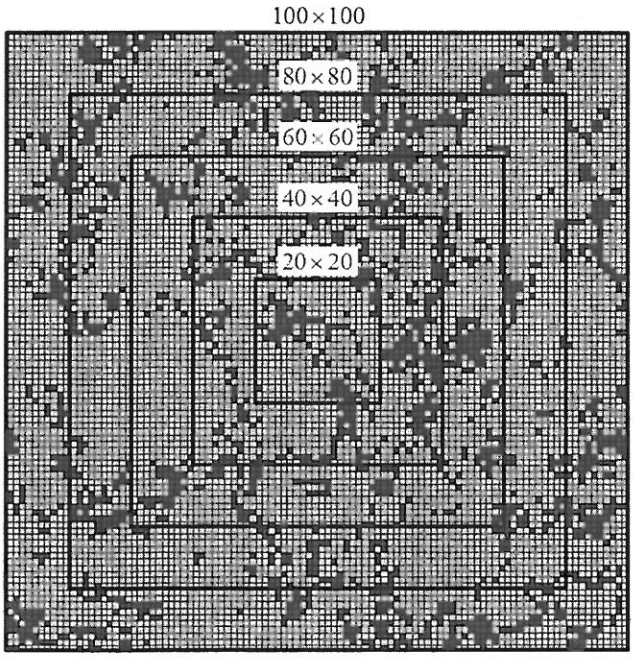

Fig. 14. Different block sizes under consideration for estimating the effective elastic properties of a material with random voids $n = 0.2$ and $\theta = 20$.

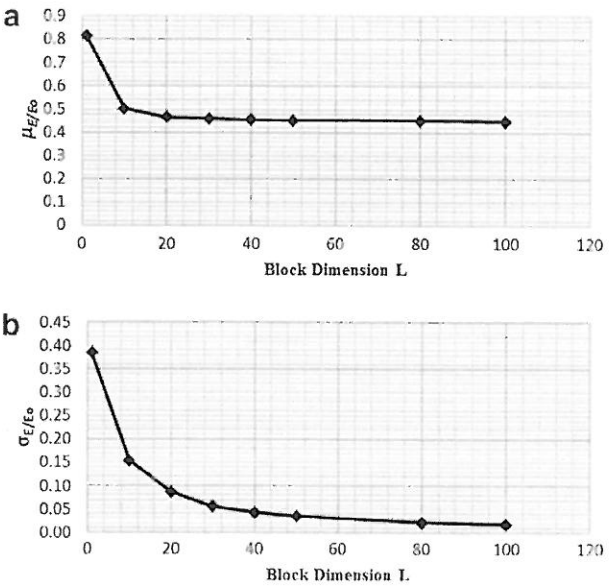

Fig. 15. Effective Young's modulus (a) mean and (b) standard deviation following 1000 simulations for different block sizes.

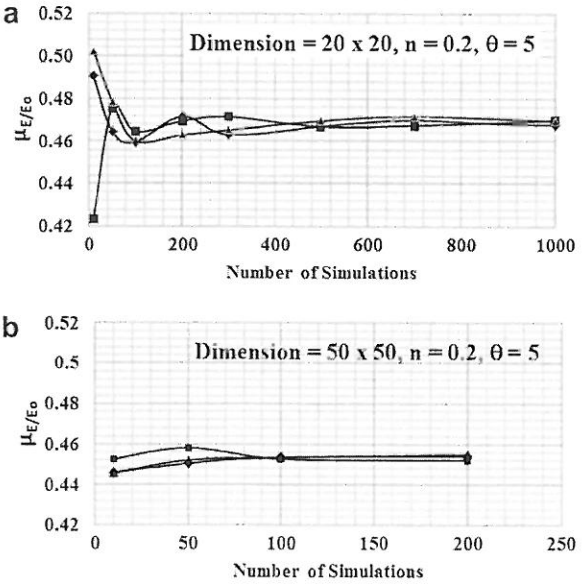

Fig. 16. Comparison of the number of simulations for convergence with different block sizes: (a) 20 × 20 and (b) 50 × 50 with $n = 0.2$ and $\theta = 5$.

This constant was then used during Monte-Carlo simulations to compute the effective Young's modulus based on the vertical footing displacement δ_{v_i} using the relationship

$$E_i = \frac{C}{\delta_{v_i}}, \quad i = 1, 2, \ldots, 1000 \tag{13}$$

As in the block tests presented earlier, the spatial correlation length did not make much difference to the mean effective stiffness in the settlement analyses. In Fig. 18, the results from the settlement and block analyses with 50 × 50 are compared for the case of $\theta = 10$ m (or $\Theta = \theta/B = 1$), and are in good agreement across a range of porosities.

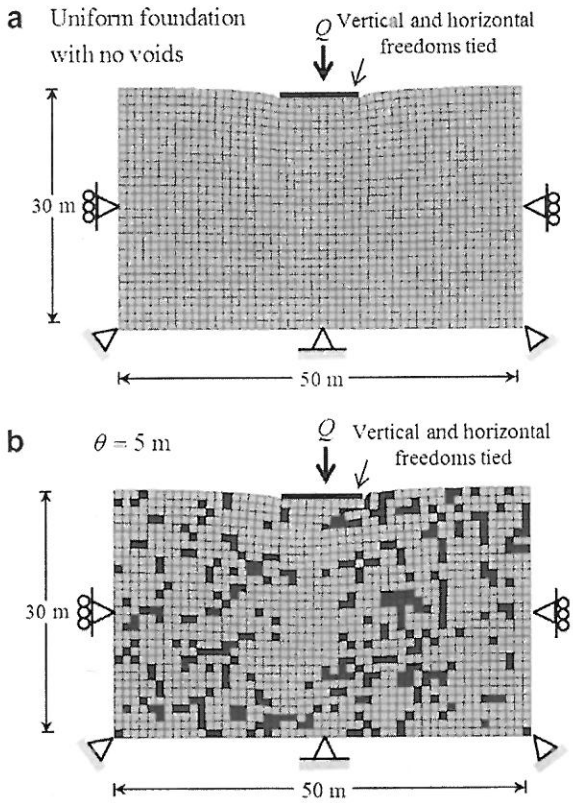

Fig. 17. Loaded strip footing supported by a material with (a) $n = 0$ and (b) $n = 0.2$ and $\theta = 5$ m.

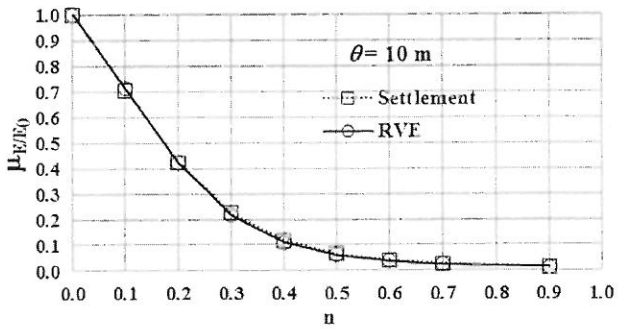

Fig. 18. Comparison of results from settlement and 50 × 50 RVE block analyses with $\theta = 10$ m.

12. Probabilistic interpretation

In order to make probabilistic interpretations from a Monte-Carlo analysis, we can count the number of simulations that exceed an allowable design value as a proportion of the total number of simulations, and/or fit a probability density function to the data as in Fig. 19. The histogram shown in the figure indicates the frequency distribution of effective Young's modulus values following a suite of 1000 Monte-Carlo simulations of the footing settlement problem. The smooth line is a fitted normal distribution based on the computed mean and standard deviation values ($\mu_{E/E_0} = 0.426, \sigma_{E/E_0} = 0.104$).

Let us assume that the design of a footing is inadequate if the settlement exceeds some critical value corresponding to $E/E_0 < 0.3$. For the particular analysis shown in Fig. 19, there are

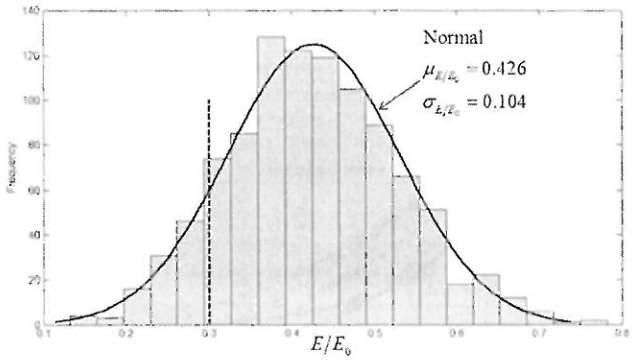

Fig. 19. Histogram of effective Young's modulus values from a settlement analysis following a suite of 1000 Monte-Carlo simulations together with a fitted normal distribution. ($n = 0.2, \Theta = 1.0$).

116 simulations that satisfy this criterion, hence with 1000 simulations we can conclude that $P[E/E_0 < 0.3] \approx 0.116$. The normal probability density function shown in Fig. 19 is seen to be a reasonable fit to the data and can also be used to predict $P[E/E_0 < 0.3]$ as follows:

Sample calculation:

(1) From Monte-Carlo simulations, $\mu_{E/E_0} = 0.426, \sigma_{E/E_0} = 0.104$.

(2) Probability of design "failure" $P[E/E_0 < 0.3] = \Phi\left[\frac{0.3 - 0.426}{0.104}\right] \approx 11\%$

where $\Phi[.]$ is the standard cumulative distribution function.

The result is close to the result obtained by counting as expected, namely that there is an 11% probability of excessive settlement.

13. Concluding remarks

The random finite element method (RFEM) shows promise as a powerful alternative approach for modeling the mechanical influence of inclusions and voids in geomaterials. Inclusions are not restricted to simple shapes as in some of the theoretical methods, and the user can control the volume and size of inclusions through changes to the spatial correlation length.

The RFEM together with Monte-Carlo simulations has been used in this study to investigate the influence of porosity and void size on the effective stiffness of geomaterials containing random voids. A novel "tied freedom" approach has been used to model an idealized block leading to predictions of the effective Young's modulus as a function of porosity and void size. It was observed that while porosity had a significant effect on effective stiffness, the void size was less important.

Results were presented demonstrating the influence of block size and the number of Monte-Carlo simulations needed to achieve stable results for a given level of porosity. As expected, more simulations were needed for smaller blocks, but the mean effective stiffness converged quite rapidly as the block size increased while the standard deviation tended to zero.

Finally, the paper presented some RFEM results relating to the settlement of a strip footing resting on an elastic foundation containing voids. It was demonstrated how these results could be used to deliver probabilistic conclusions relating to foundation settlement.

Acknowledgements

The authors wish to acknowledge the support of (i) NSF Grant CMMI-0970122 on "GOALI: Probabilistic Geomechanical Analysis

in the Exploitation of Unconventional Resources", (ii) KGHM Cuprum, Wrocław, Poland through the Framework 7 EU project on "Industrial Risk Reduction" (IRIS).

References

Benveniste, Y., 1987. A new approach to the application of Mori–Tanaka theory in composite materials. Mech. Mater. 6, 147–157.

Budiansky, Y., 1965. On the elastic moduli of some heterogeneous material. J. Mech. Phys. Solids 13, 223–227.

Christensen, R.M., Lo, K.H., 1979. Solutions for effective shear properties in three phase sphere and cylinder models. J. Mech. Phys. Solids 27, 315–330.

Cosmi, F., 2004. Two-dimension estimate of effective properties of solid with random voids. Theor. Appl. Fract. Mech. 42, 183–189.

Davis, E.H., Taylor, H., 1962. The movement of bridge approaches and abutment on soft foundation soils. In: Proceedings of the 1st Biennial Conference on Australian Road Research Board. p. 740.

Day, A.R., Snyder, K.A., Garboczi, E.J., Thorpe, M.F., 1992. The elastic moduli of a sheet containing circular holes. J. Mech. Phys. Solids 40, 1031–1051.

Der Kiureghian, A., Zhang, Y., 1999. Space-variant finite element reliability analysis. Comput. Methods Appl. Mech. 168 (1–4), 173–183.

Esmaieli, K., Hadjigeorgiou, J., Grenon, M., 2010. Estimating geometrical and mechanical REV based on synthetic rock mass models at Brunswick Mine. Int. J. Rock Mech. Min. 47, 915–926.

Fenton, G.A., Griffiths, D.V., 2008. Risk Assessment in Geotechnical Engineering. John Wiley and Sons, Hoboken, NJ.

Fenton, G.A., Vanmarcke, E.H., 1990. Simulation of random fields via local average subdivision. J. Eng. Mech. 116 (8), 1733–1749.

Garboczi, E.J., Day, A.R., 2005. An algorithm for computing the effective linear elastic properties of heterogeneous materials: three-dimensional results for composites with equal phase Poisson ratios. J. Mech. Phys. Solids 43 (9), 1349–1362.

Griffiths, D.V., Fenton, G.A., 2004. Probabilistic slope stability analysis by finite elements. J. Geotech. Geoenviron. 130 (5), 507–518.

Griffiths, D.V., Dotson, D., Huang, J., 2011a. Probabilistic finite element analysis of a raft foundation supported by drilled shafts in karst. In: Juang, H., et al. (Eds.), Proceedings of the GeoRisk 2011, ASCE Geotechnical Special Publication No. 224, (CD-ROM).

Griffiths, D.V., Paiboon, J., Huang, J., Fenton, G.A., 2011b. Numerical analysis of the influence of porosity and void size on soil stiffness using random fields. In: Khalili, N., Oeser, M. (Eds.), Proceedings of the 13th International Conference of the International Association for Computer Methods & Advances in Geomechanics (IACMAG 2011), Melbourne, Australia. Centre for Infrastructure Engineering and Safety, Sydney, pp. 21–27.

Hashin, Z., 1962. The elastic moduli of heterogeneous materials. J. Appl. Mech. 29, 143–150.

Hill, R., 1963. Elastic properties of reinforced solids: some theoretical principles. J. Mech. Phys. Solids 11, 357–372.

Hill, R., 1965. A self-consistent mechanics of composite materials. J. Mech. Phys. Solids 13, 213–222.

Hu, N., Wang, B., Tan, G.W., Yao, Z.H., Yuan, W.F., 2000. Effective elastic properties of 2D solids with circular voids: numerical simulations. Compos. Sci. Technol. 60, 1811–1823.

Huang, J.S., Krabbenhoft, K., Lyamin, A., under review. Statistical homogenization of elastic properties of later age cement paste based on X-ray microtomography images. Int. J. Solids Struct. submitted for publication.

Isida, M., Igawa, H., 1991. Analysis of zig–zag array of circular holes in an infinite solid under uniaxial tension. Int. J. Solids Struct. 27, 849–864.

Kanit, T., Forest, S., Galliet, I., Mounoury, V., Jeulin, D., 2003. Determination of the size of the representative volume element for random composites: statistical and numerical approach. Int. J. Solids Struct. 40, 3647–3679.

Klusemann, B., Svendsen, B., 2009. Homogenization methods for multi-phase elastic composites comparisons and benchmarks. Tech. Mech. 30 (4), 374–386.

Kulatilake, P.H.S.W., 1985. Estimating elastic constants and strength of discontinuous rock. J. Geotechnol. Eng. ASCE 111, 847–864.

Li, B., Wang, B., Reid, S.R., 2010. Effective elastic properties of randomly distributed void models for porous materials. Int. J. Mech. Sci. 52, 726–732.

Liu, C., 2005. On the minimum size of representative volume element: an experimental investigation. Exp. Mech. 45 (3), 238–243.

Mori, T., Tanaka, K., 1973. Average stress in matrix and average elastic energy of materials with misfitting inclusions. Acta Metall. 21 (5), 571–574.

Ning, Y., Xu, W.Y., Zheng, W.T., Meng, G.T., Shi, A.C., 2008. Study of random simulation of columnar jointed rock mass and its representative elementary volume scale. Chinese J. Rock Mech. Eng. 27 (6), 1202–1208.

Poulos, H.G., Davis, E.H., 1974. Elastic Solution for Soil and Rock Mechanics. John Wiley and Sons, New York, London, Sydney, Toronto.

Roscoe, R., 1952. The viscosity of suspensions of rigid spheres. J. Appl. Phys. 3, 267.

Smith, I.M., Griffiths, D.V., 2004. Programming the Finite Element Method, fourth ed. John Wiley and Sons, Chichester, New York.

Sudret, B., Der Kiureghian, A., 2000. Stochastic finite elements and reliability, *a state-of-the-art report*, Technical Report No. UCB/SEMM-2000/08, University of California, Berkeley.

Vanmarcke, E.H., 1984. Random Fields: Analysis and Synthesis. The MIT Press, Cambridge, Mass.